

# Improved slurry zinc/air systems as batteries for urban vehicle propulsion

P. C. FOLLER\*

*The Continental Group, Inc. Energy Systems Laboratory†, 10432 N. Tantau Avenue, Cupertino, California 95014, USA*

Received 29 November 1982; revised and permission to publish received 28 December 1985

Traditionally having been attractive for side-stepping the difficulties of secondary zinc anodes and bifunctional air-cathodes, slurry zinc/air cells are shown to be capable of higher powers than previously thought. Coupling advances in air-cathode manufacture, separator selection and cell design, these results prompted a characterization of electrolyte discharge capacity and self-discharge, as well as on-board and central recharge schemes. Projections of overall efficiency and performance are made (along the lines of the 1975 CGE-SAFT 15 kW battery) to full-scale primary and secondary systems comprising 30% the weight of 1000 kg vehicles. The problems to be resolved in development are discussed and are shown not to seriously detract from the potential of this couple as a prime candidate for electric vehicle propulsion.

## 1. Introduction

### 1.1. *The rationale for the development of slurry zinc/air systems*

The development of all secondary batteries utilizing planar zinc as the positive electrode has progressed slowly due to morphological problems in electrodeposition and shape-change phenomena on cycling. The development of zinc/air systems utilizing planar electrodes also faces the additional problems of bifunctional air-electrodes in secondary design, or rapid-refuelability in primary configurations.

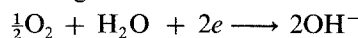
The slurry system side-steps these issues and exhibits the conveniences of rapid mechanical recharge and sustained peak power capability, along with a potentially high cycle life and low cost. Electrochemical recharge may be readily accomplished in separate cells. A mixture of dendritic and mossy zinc particulates may be electrodeposited over a wide range of conditions onto substrates to which they do not adhere. Self-discharge losses are low despite the high zinc surface area. Overall electric-to-electric

efficiency is among the highest of metal/air systems.

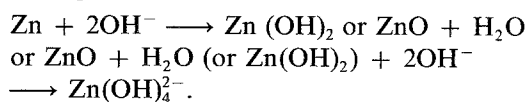
### 1.2. *Chemical and electrochemical reactions*

The chemical and electrochemical reactions of slurry zinc/air cells in silicate-extended 12 mol dm<sup>-3</sup> KOH electrolyte may be summarized as follows:

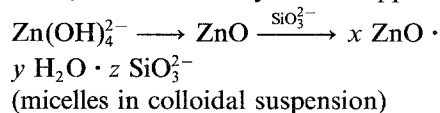
Discharge at cathode:



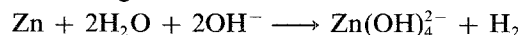
Discharge at anode:



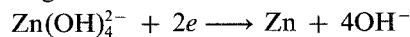
Then, as the solubility limit is approached:



Self discharge:



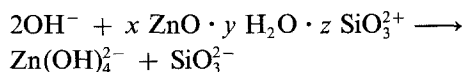
Charge at cathode:



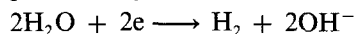
solubilizing the colloid:

\* Present address: OxyTech, Inc., 10432 N. Tantau Avenue, Cupertino, CA 95014, USA.

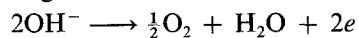
† Laboratory disbanded 31 December 1981, Continental Group acquired by Kiewit-Murdoch, 1984.



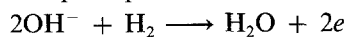
parasitically:



Charge at anode. There are two possibilities:



and perhaps in central recharge:



The possibility of oxidizing hydrogen instead of the anodic evolution of oxygen substantially changes the overall energy use economics of slurry zinc/air electric vehicles. If primary resource-derived hydrogen can be used, the severe loss encountered in electric power generation can be partially bypassed and the poor kinetics of the oxygen evolution reaction are eliminated.

*1.2.1. Discharge cell design.* Discharge cells for slurry zinc/air systems may be constructed in several geometries broadly classified as either planar or tubular. The electrode materials in either are layered as follows, proceeding from the electrolyte side to the air side:

1. The anodic current collector. A fine copper exmet is usually chosen, due to corrosion resistance, and a 'surface-alloying' with discharging zinc.

2. The separator. Asbestos had been used to increase the bubble pressure of the air-cathodes. If this is unnecessary, extremely open felts or meshes of polymeric materials have advantages in resistivity (openings must be smaller than the average zinc particle size).

3. The air-cathode. Teflon-bonded and catalysed high area carbons pressed into current collection exmets work well. The sensitive active layer is thus rigidly sandwiched between the expanded metal of the anodic and cathodic current collectors.

The performance of the discharge cells is greatly influenced by the tightness of the cell sandwich and by placement of anode and cathode busses. Tubular geometry has the advantage of readily achieving compression and minimizing zinc settling, but requires additional bus-bar length if high-performance state-of-the-art air-cathodes are used. Figure 1 presents two

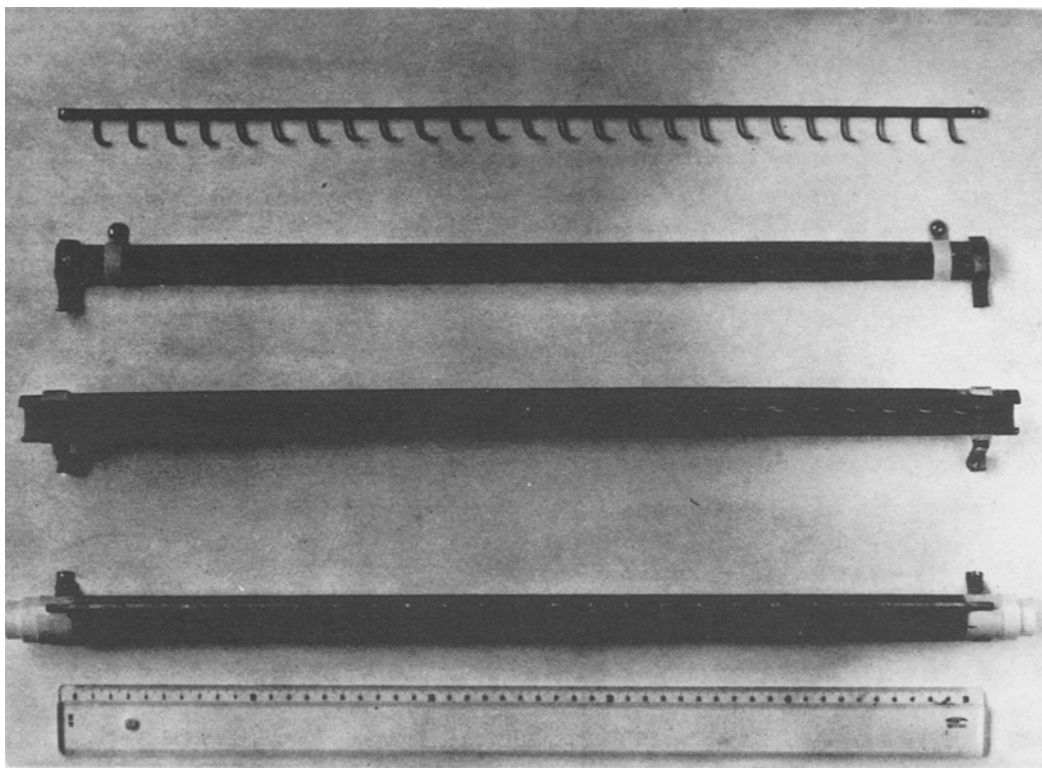


Fig. 2. Construction of a 1975 Compagnie Generale d'Electricité charge tube.

coupled 'modules' of discharge tubes constructed by the Compagnie Generale d'Electricité (and affiliate SAFT) during their development effort of the early 1970s.

*1.2.2. Charge cell design.* Slurry zinc/air batteries have been regarded by most developers as primary systems, the spent electrolyte being reprocessed by chemical rather than electrochemical means. Consequently, charge cell designs are not highly developed. Particulate zinc may be readily electrodeposited onto magnesium cathodes without real adherence. Electrolyte flow has then been used to strip cathodes in both planar geometry and in a geometry wherein  $1 \text{ mm}^2$  Mg tips are placed axially in a tubular oxygen-evolving anode. This latter measure was taken to achieve higher reliability in zinc removal but suffered from low current efficiency and high cell voltage over the initial third of each 7–10 minute deposition cycle. Figure 2 illustrates the construction of the charge tubes developed by Compagnie Generale d'Electricité

in 1975. Scraped rotating cylinders are also an attractive option for powder deposition.

### *1.3. Prior development programmes and critical issues raised*

Over the last few years there have been of the order of ten independent investigations of the use of the zinc/air couple for vehicle propulsion. The majority of the work has been in planar electrode systems and may be represented by the primary systems of General Motors [1] ( $55 \text{ W kg}^{-1}$ ,  $99 \text{ Wh kg}^{-1}$ ) and that of General Atomics [2] and Toyota [3].

Circulating slurry batteries have been built by Sony [4], Sanyo [5], the Bulgarian Academy of Sciences [6], and the Compagnie General d'Electricité (CGE) [7–10]. Several patents dealing with such systems have appeared [11–13]. Also, a paper study was undertaken [14].

Poor power output has been a characteristic of all the circulating systems except that of CGE, who cite  $80 \text{ W kg}^{-1}$ . For instance, the Sony

system was only capable of  $24 \text{ W kg}^{-1}$ . In the case of the Bulgarian work, several factors contributed to low performance. These were: low KOH concentration, absence of colloidal discharge product suspension agents, ambient temperature and a fairly low zinc content in the slurry due to settling problems in their planar cell design.

It is generally agreed that the investigation of CGE produced the most advanced slurry zinc/air systems to date. Units of up to  $15 \text{ kW}$  were built over the five year programme. Thus, the design of this system was used for the scale-up projection of the results of the present study. Using the methodology of these projections, the performance of the 1975 CGE system (in full,  $300 \text{ kg}$  size) works out to  $82 \text{ W kg}^{-1}$  and  $84 \text{ Wh kg}^{-1}$ .

The common problem in previous studies of the slurry zinc/air system has been the poor performance of the air-cathodes and consequent cell stack weight requirements. It now appears that improvements are possible.

## 2. Demonstrated and proposed improvement areas

Slurry zinc/air systems may be improved by the incorporation of state-of-the-art air-cathode formulations. Recent interest in the application of air-cathode technology to chlor-alkali cells has led to the development of high-rate formulations of reduced catalytic content. As will be shown, even off-the-shelf air-electrode formulations can provide outstanding power capability in small slurry zinc/air cells.

Advances in discharge cell design can allow the higher levels of power now available to be collected with acceptable IR loss. Improved separator selection, and the use of bus-bars in tubular geometry can reduce such losses. With the use of bus-bars, overall current collector weight can be reduced because lighter current collection exmets can be used in the cell 'sandwich' itself. Such current collection improvements may be calculated simply and have been used in the scale-up modelling discussed later.

It was obvious that planar or cylindrical electrode charge cells would be desirable, if practical, because of periodic high cell voltages and

low current efficiencies in the previously advanced (CGE) tip-and-tube charger geometry. Deposit adherence and morphological characteristics in planar geometry at controlled and constant power consumption were, indeed, found to be acceptable and consistent with mechanical removal techniques.

The low efficiency of zinc/air battery systems arises from the poor kinetics of the oxygen-reducing electrode and, in secondary systems, the evolution of oxygen on recharge, another notoriously slow process. Elimination of oxygen evolution by substituting the oxidation of hydrogen was found to cut overall energy consumption by approximately half.

Favourable operating cost economics are a consequence. Utilizing hydrogen depolarized recharge is only possible in mechanically rechargeable systems and, of these, the slurry zinc anode is most suited. Though it is not economic to transport zinc slurry because its energy content is too low, it is conceivable that it can be distributed back to vehicles at the site of collection and recharge. A dispersed network of smaller-scale recharge service stations may thus be envisioned.

## 3. Discharge results

To evaluate the performance characteristics of slurry zinc/air cells equipped with state-of-the-art air-cathodes and separators of maximum open area, two cells were built.

A  $3 \text{ cm}^2$  cell was used to rapidly characterize various cathodes, separators and anode exmets. It was formed of discs of these materials sealed onto the end of an air tube by a threaded cap. The cell was then hung in a beaker of electrolyte, wherein suspension of zinc was achieved through magnetic stirring. A  $55^\circ \text{ C}$  electrolyte of  $12 \text{ mol dm}^{-3}$  KOH with the addition of silicate ion to the extent of  $25 \text{ g SiO}_2$  per litre was used in all cases. In this,  $300 \text{ g}$  of  $100$  mesh Zn was suspended, and so such testing is only representative of  $100\%$  state-of-charge. Performance curves were developed through increasing resistive load over approximately  $5 \text{ min}$  intervals.

A particularly convenient aspect of the  $3 \text{ cm}^2$  cell design was the ability to tailor both air

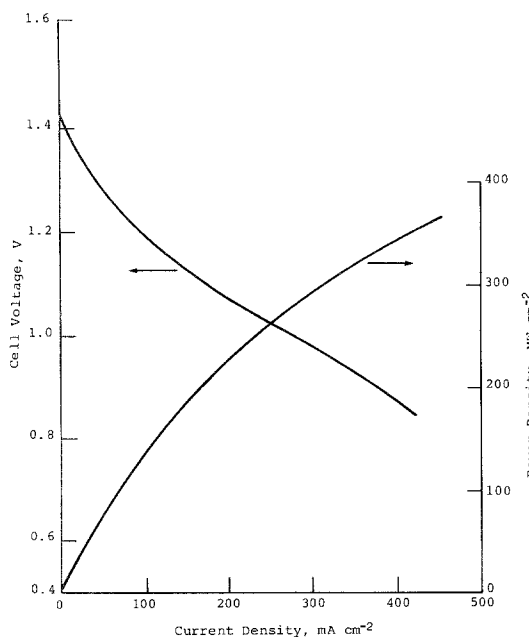


Fig. 3. Performance of  $3\text{ cm}^2$  cell using an off-the-shelf  $3.0\text{ mg Pt cm}^{-2}$  cathode of manufacturer 'A'.  $55^\circ\text{C}$ ,  $12\text{ mol dm}^{-3}\text{ KOH} + 25\text{ g dm}^{-3}\text{ SiO}_2 + 300\text{ g dm}^{-3}\text{ 100 mesh Zn}$ .

backpressure and electrolyte pressure (cell depth) to optimize cathode performance.

Figure 3 shows the cell voltage and power curves of the  $3\text{ cm}^2$  cell using a  $3.0\text{ mg Pt cm}^{-2}$  cathode of a manufacturer denoted 'A'. This cathode was originally developed for use in chlor-alkali cells. Though well below the peak, the highest power measured was  $360\text{ mW cm}^{-2}$ .

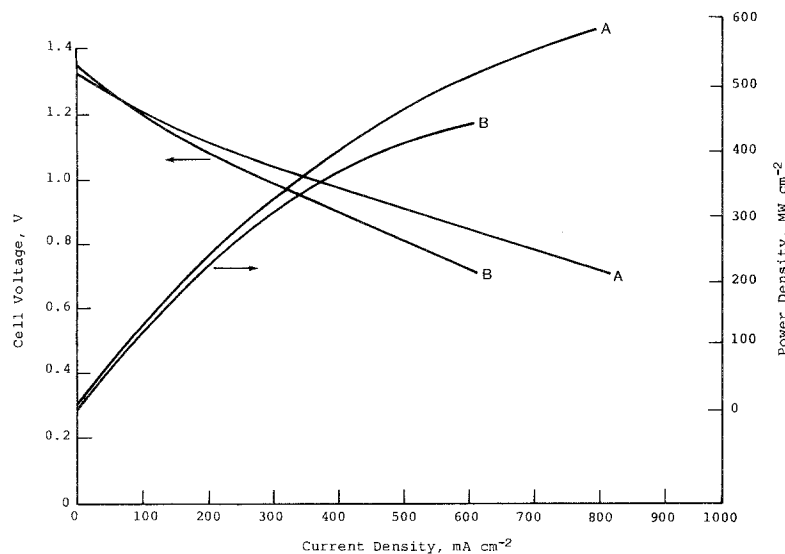


Fig. 4. Performance of  $3\text{ cm}^2$  cell using a specially designed cathode of manufacturer 'A' ( $0.4\text{ mg Pt cm}^{-2}$ ), and an off-the-shelf cathode of manufacturer 'B' ( $0.33\text{ mg Pt cm}^{-2}$ ).  $55^\circ\text{C}$ ,  $12\text{ mol dm}^{-3}\text{ KOH} + 25\text{ g dm}^{-3}\text{ SiO}_2 + 300\text{ g dm}^{-3}\text{ 100 mesh Zn}$ .

In most cases measurement was terminated near  $450\text{ mA cm}^{-2}$  as beyond this point additional current collection is not weight effective in a tubular cell geometry.

In Fig. 4 it is shown that cathodes containing an order of magnitude less catalyst can outperform the system illustrated in Fig. 3. A maximum power of over  $550\text{ mW cm}^{-2}$  was observed at  $800\text{ mA cm}^{-2}$  with careful control of air and electrolyte pressure. This cathode was designed for operation in  $12\text{ mol dm}^{-3}\text{ KOH}$  electrolyte. The cathode 'B' of Fig. 4 was an 'off-the-shelf' formulation for chlor-alkali cells.

The peak powers exhibited in the  $3\text{ cm}^2$  experimentation are the highest yet reported for zinc/air cells. On oxygen, peak powers of nearly  $1000\text{ mW cm}^{-2}$  have been observed in our studies.

A  $100\text{ cm}^2$  cell was constructed in order to test performance at a more realistic size and to couple with an electrolyte reservoir of a low enough volume such that electrolyte compositions could be fully discharged in 4–5 h periods. The cell was of flat configuration, having three electrolyte channels. Electrolyte was pumped up the central channel and allowed to cascade down the outboard channels. A throttled centrifugal pump was used to control flow rate.

Figure 5 compares the performance achieved in the  $100\text{ cm}^2$  cell at a temperature of  $55^\circ\text{C}$ . Performance somewhat below that in the  $3\text{ cm}^2$

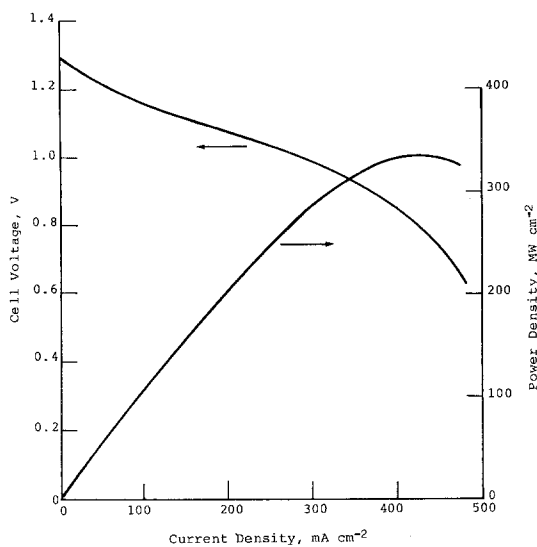


Fig. 5. Performance of  $100\text{ cm}^2$  cell using an off-the-shelf cathode of manufacturer 'C',  $0.4\text{ mg Pt cm}^{-2}$ .  $55^\circ\text{C}$ ,  $12\text{ mol dm}^{-3}\text{ KOH} + 25\text{ g dm}^{-3}\text{ SiO}_2 + 350\text{ g dm}^{-3}$  100 mesh Zn.

cell was found. Possible explanations include insufficient 'tightness' of the cell sandwich over the large area (contributing to IR losses) and the inability in this system to adjust electrolyte pressure to achieve optimal performance. A peak power of  $330\text{ mW cm}^{-2}$  was observed. A maximum of  $255\text{ mW cm}^{-2}$  was observed in the  $320\text{ cm}^2$  tubular cells tested by CGE in 1975.

It is clear much higher levels of performance can be achieved with optimized cathodes and improved methods of cell construction.

One of the attractive features of slurry zinc/air systems, and, indeed, all flow batteries, is that peak powers may be sustained over substantial

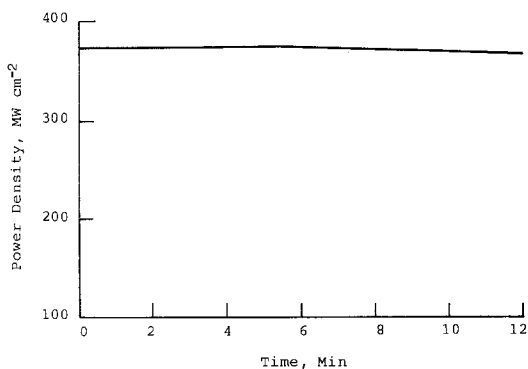


Fig. 6. Demonstration of sustained peak power capability.  $3.0\text{ mg Pt cm}^{-2}$  cathode manufacturer 'A'.  $12\text{ mol dm}^{-3}\text{ KOH} + 25\text{ g dm}^{-3}\text{ SiO}_2 + 300\text{ g dm}^{-3}$  100 mesh Zn.

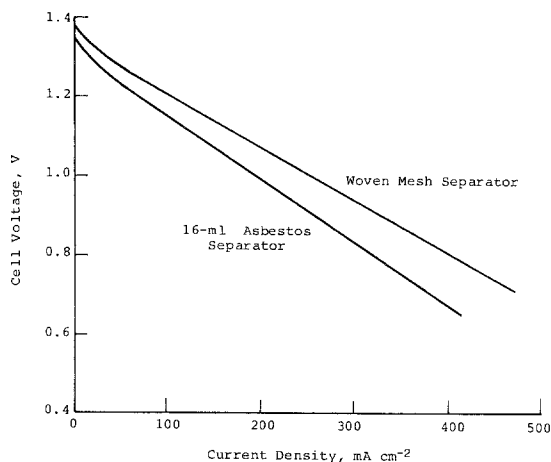


Fig. 7. Improved performance of  $3\text{ cm}^2$  cell using woven mesh separator.  $3.0\text{ mg Pt cm}^{-2}$  cathode manufacturer 'A'.  $55^\circ\text{C}$ ,  $12\text{ mol dm}^{-3}\text{ KOH} + 25\text{ g dm}^{-3}\text{ SiO}_2 + 300\text{ g dm}^{-3}$  100 mesh Zn.

periods of time. Figure 6 illustrates this with the  $3.0\text{ mg Pt cm}^{-2}$  cathode of Fig. 3. The experiment was voluntarily terminated after 12 minutes of a constant  $370\text{ mW cm}^{-2}$ .

The experimental cells of Figs 3–6 were constructed using identical separators and anode current collector exmet grid size. To illustrate the improvement available by using extremely open separators (as was carried out) versus using asbestos (which is sometimes thought desirable as a gas barrier in air-cathode design) the comparison of Fig. 7 was performed. As much as a  $100\text{ mV}$  difference at  $400\text{ mA cm}^{-2}$  is seen when 40% open ( $\neq 100$ ) 7 mil woven polypropylene meshes are used.

### 3.1. Electrolyte discharge capacity

The energy density of the slurry zinc/air system is determined by the amount of zinc that may be discharged into the electrolyte. As in studies of anodic passivation at planar electrodes, several physical parameters are influential. Electrolyte flow rate and viscosity are important to the transport of  $\text{OH}^-$  to the electrode surface and  $\text{Zn}(\text{OH})_4^{2-}$  away from it. KOH concentration influences ultimate zincate solubility as well as mass transport. Of more importance than its equilibrium solubility, significant levels of super saturation of zincate are commonly observed in the anodic dissolution of zinc. Exhibiting

extraordinary stability, levels over double the equilibrium concentration may be sustained over periods of months [15].

Current density is a crucial parameter in studies of passivation phenomena. In the slurry system this parameter has little quantitative meaning, but is quite important still, in that current density based on cell area does influence discharge capacity: the higher the current density the lower discharge capacity in constant current experiments. Not surprisingly, anode current collector mesh size also influences discharge capacity (opening up the mesh or lightening the battery decreases discharge capacity).

In the slurry system the method of electrolyte pumping is also of influence. It is the shearing flow of electrolyte on suspended particulates that aids in discharge product dissolution. Using severely throttled centrifugal pumps, greater discharge capacities are observed. Flexible impeller pumps actually abrade discharge product from the particulates thus increasing discharge capacity.

In the following experiments a centrifugal pump was used to maintain a constant flow rate. The electrolytes were variations on a  $12 \text{ mol dm}^{-3}$  KOH base at  $55^\circ \text{C}$ . Zinc was present to the extent of  $300 \text{ g dm}^{-3}$  of 100 mesh powder. A constant current density of  $150 \text{ mA cm}^{-2}$  was

maintained using an anodic current collector of identical mesh size in all cases.

The electrolyte discharge capacities of up to  $220 \text{ Ah dm}^{-3}$  reported by CGE-SAFT were not obtained in the following experiments due to operation at higher current density ( $80 \text{ mA cm}^{-2}$  was used in the former work).

Figure 8 shows the constant current discharge curves of  $12 \text{ mol dm}^{-3}$  KOH electrolyte and  $12 \text{ mol dm}^{-3}$  KOH with the addition of the silicate ion expressed as  $28 \text{ g dm}^{-3}$  of  $\text{SiO}_2$ . Silicate can increase discharge capacity by over a factor of two.

The usual explanation of this extraordinary effect is that the silicate ion adsorbs on  $\text{ZnO}$  or  $\text{K}_2\text{Zn}(\text{OH})_4$  nuclei, imparting a strong negative charge [16]. Repulsion of these nuclei results in the formation of a 'quasi-colloid'. It is best called a quasi-colloid as it slowly agglomerates over a period of weeks, turning an initially black liquid into a white, translucent supernatant with a black precipitate. Initially it is unfilterable, but in a matter of weeks may be substantially clarified by filtration.

Figure 9 presents the results of a study of silicate ion concentration. It is clear that a maximum is defined. The resultant electrolyte in each of the silicate experiments is black and colloidal, rather than the clear, though choked with white

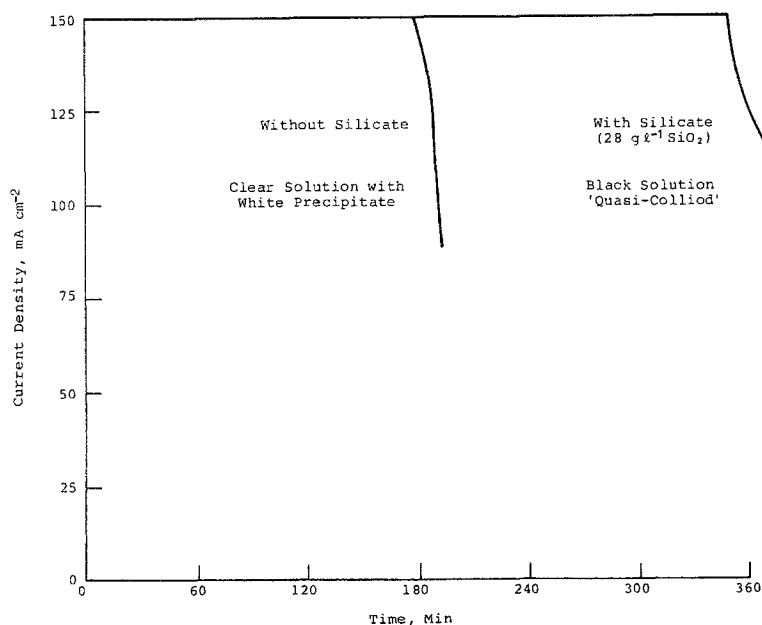


Fig. 8. Effect of silicate ion concentration on electrolyte discharge capacity.  $55^\circ \text{C}$ ,  $12 \text{ mol dm}^{-3}$  KOH +  $25 \text{ g dm}^{-3}$   $\text{SiO}_2$  +  $300 \text{ g dm}^{-3}$  100 mesh Zn,  $150 \text{ mA cm}^{-2}$ .

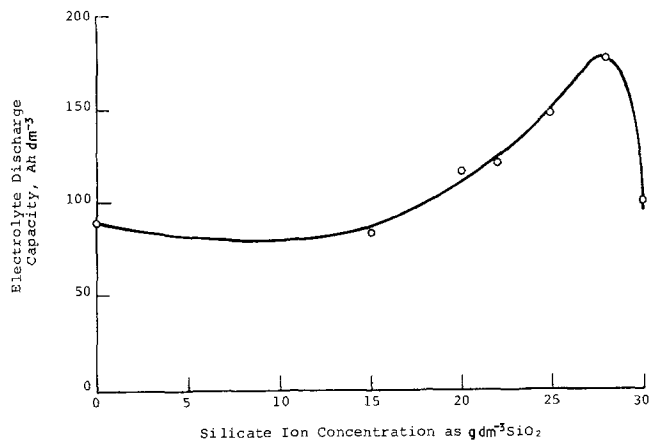


Fig. 9. Effect of silicate ion concentration on electrolyte discharge capacity. Conditions as Fig. 8.

precipitate, product in the case of  $12 \text{ mol dm}^{-3}$  KOH alone. At the  $30 \text{ g SiO}_2 \text{ dm}^{-3}$  level the presence of silicate significantly increases electrolyte viscosity. This may lead to earlier passivation. Alternately, if too thick a layer of silicate is adsorbed on the zinc electrode surface, transport of  $\text{OH}^-$  to the surface may be hindered or the effect surface concentration actually reduced (which would also lead to passivation). Such transport arguments also seem to apply to the dissolution of ZnO in KOH with and without a silicate addition; less ZnO dissolves in the presence of silicate over the entire spectrum of KOH concentration [17].

Silicate is apparently not the only addition agent capable of producing black colloidal suspensions of discharge product. Divalent oxyanions of the  $s^2p^2$  and  $d^2s^2$  elements (that do not chemically react, e.g. stannate, titanate) have shown this ability in initial testing [17].

## 4. Charge results

### 4.1. General findings

In alkaline electrolyte over a wide range of hydroxide ion from  $3 \text{ mol dm}^{-3}$  to  $12 \text{ mol dm}^{-3}$  and zincate ion concentration from 10 to  $300 \text{ g dm}^{-3}$  Zn it is possible to electrodeposit zinc in a mixture of mossy and dendritic morphology. So long as one operates in a diffusion-controlled regime (that is, at high fractions of limiting current, or above limiting current) a mostly dendritic morphology results. At lower fractions of limiting current moss predominates and deposits are more compact in character. Figure 10 presents the size distribution of the powder deposited from  $12 \text{ mol dm}^{-3}$  KOH containing  $50 \text{ g dm}^{-3}$  Zn at  $150 \text{ mA cm}^{-2}$ . This distribution is fairly insensitive to experimental parameters probably due to the ease with which dendrites are broken

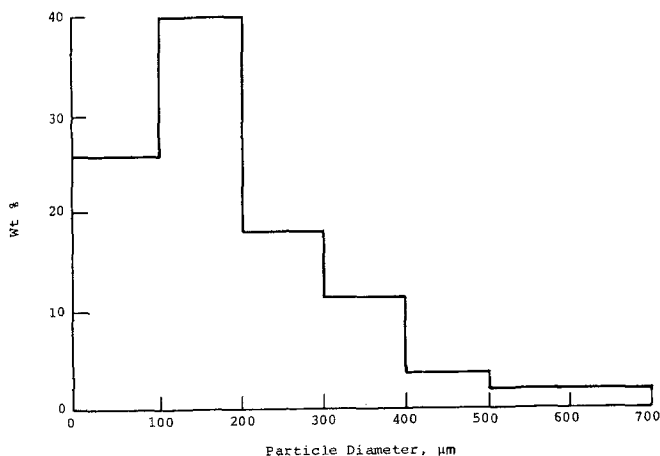


Fig. 10. Size distribution of zinc powder electrodeposited in planar geometry cells.  $50 \text{ g dm}^{-3}$  Zn as zincate,  $25^\circ \text{C}$ ,  $12 \text{ mol dm}^{-3}$  KOH +  $25 \text{ g dm}^{-3}$   $\text{SiO}_2$ ,  $150 \text{ mA cm}^{-2}$ .



at the nodes in their regular structure. Deposits of zinc onto magnesium cathodes are readily removed probably due to the cathode's persistent oxide coverage. Adherence is quite weak; however, to guarantee 100% removal (to avoid shorting on subsequent cycles) cell design is somewhat complicated.

In the 'tip-and-tube' geometry designed in 1975 by CGE-SAFT (Fig. 2), zinc is electrodeposited onto the exposed ends of magnesium wires of  $1 \text{ mm}^2$  area. A row of such tips is placed axially within a cylindrical oxygen-evolving anode. Every 7–10 minutes a pulse of electrolyte flow is applied to remove nodules of electrodeposit. A brief period at open circuit then reconditions the magnesium surface.

Current efficiency in tip-and-tube geometry is poor, primarily due to the initially very high current density that is applied to each tip. At the 8 h charge rate of 1 A per tip several tens of amperes per square centimetre are passed. As the zinc deposit grows, current density decreases and current efficiency improves. Still, over the initial third of each 7–10 min deposition cycle, much hydrogen is evolved. As less and less zinc is present in the electrolyte, current efficiency worsens. Overall, an 80% current efficiency was cited by CGE for the tip-and-tube geometry integrating over zincate concentration and the deposition/removal cycles.

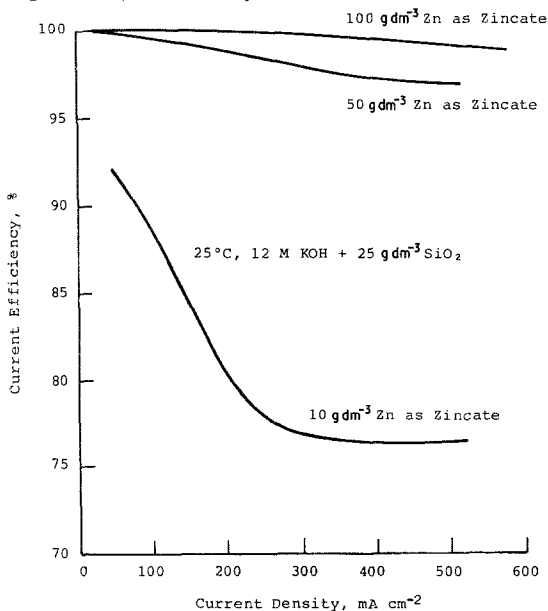


Fig. 11. Recharge current efficiency in planar geometry cells.

Figure 11 presents the current efficiencies which may be achieved in planar or cylindrical geometries at several levels of zincate concentration. Without forced convection it is apparent that current efficiencies of nearly 100% are possible at deposition rates below  $150 \text{ mA cm}^{-2}$  (based on initial surface area).

Cell voltage in tip-and-tube geometry also suffers time-dependent variation. Initially, at high current densities imposed on each tip, cell voltage can rise above 7 V. As the zinc surface area is built up, this decreases. In tip-and-tube geometry cell voltage remains at fairly high levels due to the large inter-electrode gap necessary for nodule growth (1 cm in the 1975 CGE cells). Figure 12 shows that cell voltage in the planar electrode geometry exhibits no time-dependent variation. Figure 12 assumes an 8 h charging rate (recharging 275 g of zinc from each litre of spent electrolyte).

The energy efficiency of the charging process may be improved through better cell design, though the disadvantages of mechanical deposit removal devices must be suffered.

#### 4.3. Use of hydrogen depolarization

The hydrogen electrode is well known for its good kinetics. It was realized that by replacing

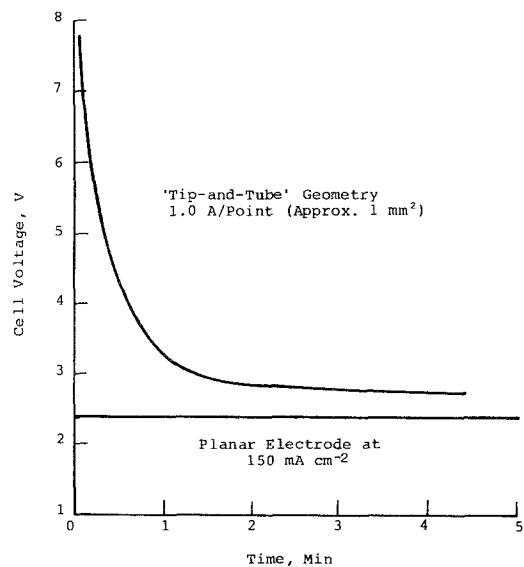


Fig. 12. Comparison of cell voltages of tip-and-tube and planar geometry recharge cells.

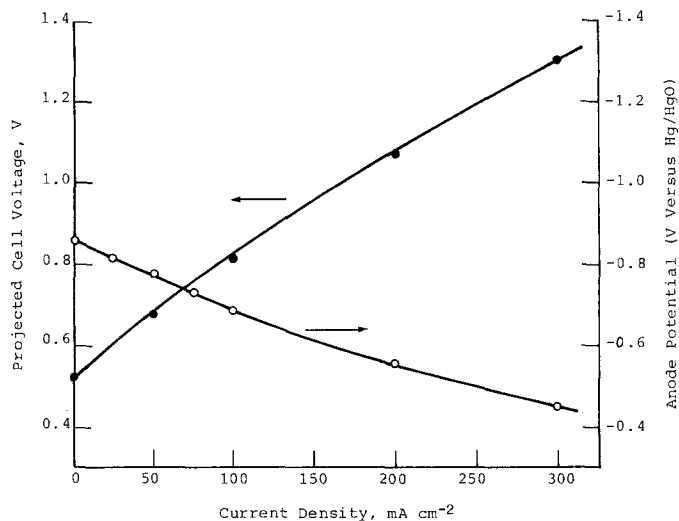


Fig. 13. Anode potential and cell voltage in hydrogen-depolarized zinc electro-deposition.  $150 \text{ g dm}^{-3}$  Zn as zincate.  $55^\circ \text{C}$ ,  $12 \text{ mol dm}^{-3}$  KOH.

oxygen evolution, a process of substantial over-voltage, approximately  $1.5 \text{ V}$  may be saved at zinc deposition rates near  $100 \text{ mA cm}^{-2}$ .

Figure 13 presents Prototech Company (Newton Highlands, MA, USA) preliminary results on hydrogen anode potential in ZnO-saturated  $12 \text{ mol dm}^{-3}$  KOH [18]. These experimental values were then used to extrapolate a cell voltage for zinc deposition. As indicated on the figure, a cell voltage of  $0.76 \text{ V}$  at  $75 \text{ mA cm}^{-2}$  is possible.

The implications of the use of the oxidation of

hydrogen as an anodic process during charge will be discussed subsequently.

### 5. Self-discharge

The corrosion of 100 mesh zinc powder in various KOH concentrations under static and operational conditions was performed in order to estimate the magnitude of this loss. Conditions of three hours in suspension at  $55^\circ \text{C}$ , and four days at the bottom of a reservoir were chosen as representative of an actual driving

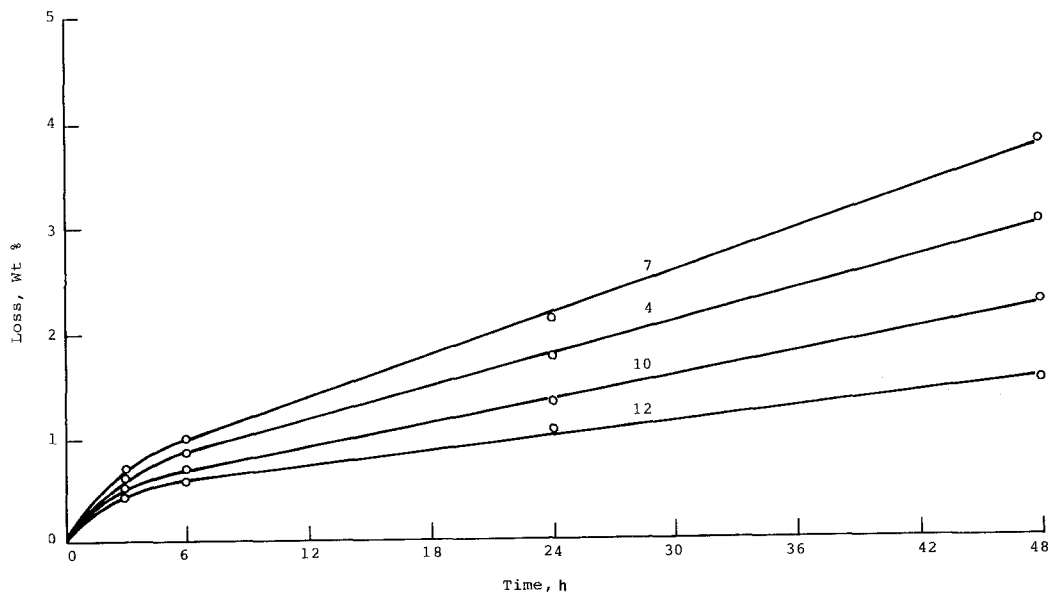


Fig. 14. Corrosion of zinc under slurry conditions,  $55^\circ \text{C}$ ,  $300 \text{ g dm}^{-3}$  100 mesh Zn. Values on lines  $\text{mol dm}^{-3}$  KOH.

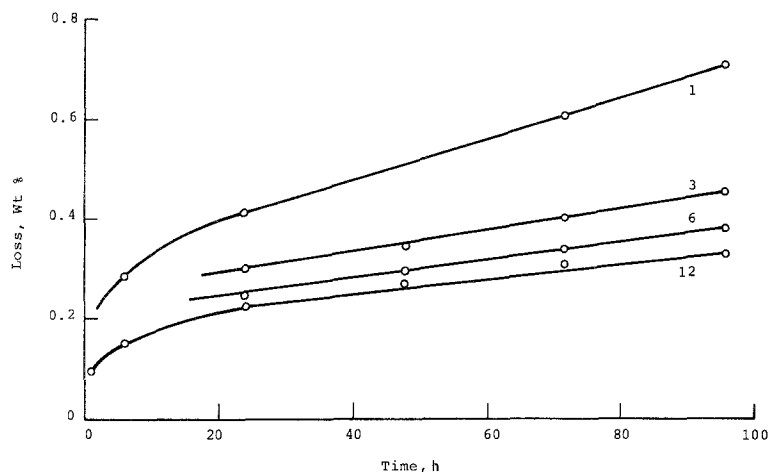


Fig. 15. Corrosion of zinc under static conditions, 25°C, 10 g dm<sup>-3</sup> SiO<sub>2</sub> + 300 g dm<sup>-3</sup> 100 mesh Zn. Values on lines mol dm<sup>-3</sup> KOH.

cycle. Analysis for zinc was performed by ICP Emission Spectroscopy. Figure 14 presents the corrosion of zinc as a percentage weight loss from the samples of 300 g Zn dm<sup>-3</sup> slurry at 55°C. Corrosion apparently decreases at higher concentrations of KOH. A loss of 0.4% is seen over a three hour period in 12 mol dm<sup>-3</sup> KOH.

In Fig. 15 it is shown that under static conditions at 25°C, approximately 0.3% weight loss is found in 12 mol dm<sup>-3</sup> KOH over 4 days.

Combined, a loss of < 1% should be expected under typical use conditions. Such a level is negligible for practical purposes.

## 6. Projection of vehicle-size performance

In order to extrapolate the performance of full-scale systems from the laboratory exploration undertaken, a mathematical model was constructed based on the 1975 CGE-SAFT 15 kW prototype, a tubular cell system. Several assumptions were needed as to electrode performance, current collection and electrolyte discharge capacity. Conventional assumptions of 30% the weight of a 1000 kg vehicle, and an average power of 11 kW required at 'cruise' were made.

The first step of the analysis was to compile the weights and volumes of all components of the full-scale battery system. This was done under the headings of discharge cells, air system, electrolyte system and optional charge cells. Thus, primary and secondary systems could be analysed. Table 1 details system weights.

The weight of each tubular discharge cell lies somewhat under that achieved by CGE, (190 versus 255 g), though the same physical dimensions are used. The revised tube uses one wrapping of fine expanded metal coupled with a bus-bar running its length for both the anodic collector and the cathodic collector. Wrappings of coarse exmet are eliminated and, thus, combined with a polypropylene mesh separator rather than asbestos the overall tube weight is reduced.

The cross-sections of the interior (copper) and exterior (nickel-plated aluminium) bus-bars were calculated to optimize the power density of the individual tube itself. The optimization traded-off additional bus-bar cross-section (weight) versus millivolts of IR loss saved. Approximate solutions gave cylindrical cross-sections of 0.25 cm<sup>2</sup> in the case of the anodic bus-bar and 0.40 cm<sup>2</sup> for the cathodic. The lower conductivity of aluminium (selected to save weight) produces a large cross-section requirement on the air side. The revised tubes were then coupled into 12-tube modules using bend tubes of the same weight as in the 1975 system. Twenty-four such modules then produce a system of reasonable power and convenient electrical and hydraulic coupling characteristics.

The air system was modelled along the same lines as that given in an analysis of the aluminium/air battery [19] whose development is being led by the Lawrence Livermore National Laboratory. Provisions for air humidification and CO<sub>2</sub> removal are included.

Table 1. Weights of battery components

Component	Weight (kg)
<i>Discharge cells (Tubular geometry)</i>	
1 Tube	0.190
12 Tube module	2.594
24 Modules + busses	63.86
<i>Air system</i>	
Intake funnel	0.2
Filter and housing	1.0
Humidifier/scrubber	1.0
Shroud	2.1
Water tank	0.38
Valves	1.5
Air pump	2.5
<i>Electrolyte system</i>	
100 dm <sup>-3</sup> tank	7.2
4 Electrolyte pumps	8.2
Inter-modular plumbing	1.2
Valves	2.2
<i>Charges</i>	
Mg cathodes	3.45
Ni anodes	6.05
Framing	0.75
Busses	0.40
Zn removal system	2.0
<i>Miscellaneous</i>	
Controls, sensors, mountings	10.0
Oxygen gained	0-6.3 (average 3.1)
Total (primary)	102.5
Total (secondary)	117.3

The power and energy densities of slurry zinc/air systems are nearly decoupled as in fuel cells. Energy (or range) is determined by the amount of zinc slurry electrolyte carried and the discharge capacity of the electrolyte. A 12 mol dm<sup>-3</sup> KOH electrolyte with the addition of 28 g dm<sup>-3</sup> SiO<sub>2</sub> (forming the silicate ion) was chosen. In this, 350 g dm<sup>-3</sup> of zinc is present.

Electrolyte discharge capacity is a function of discharge rate. The experiments performed at the Energy Systems Laboratory were not run at the 80 mA cm<sup>-2</sup> current density cited by CGE as producing 220 Ah dm<sup>-3</sup>. A capacity of 175 Ah dm<sup>-3</sup> was, however, confirmed at 150 mA cm<sup>-2</sup>. The higher CGE figure was nevertheless used for the purposes of the model.

In the model, electrolyte weight was added to that of the cells and auxiliaries to produce a

300 kg system. The capacity is thus determined given 220 Ah dm<sup>-3</sup> and 1.18 V at 80 mA cm<sup>-2</sup> (producing an average power level of 11 kW). The reservoir tank construction assumed a rectangular design and walls of 5 mm thick polypropylene. Four 1/10 hp 30 gallon min<sup>-1</sup> centrifugal pumps are used, each with their own motor and each servicing six modules through a manifold.

### 6.1. Primary and secondary systems

The batteries modelled in Fig. 16 are composed of 24 modules of 12 tubes each. Using the assumptions as to cell voltage, current density and current collection outlined in the preceding section, a system of 37 kW power results.

To the weight of these 24 modules and auxiliaries, increasing amounts of electrolyte weight and tankage (or capacity, kWh) were added. From the total weight, specific power and specific energy were calculated. Thus Fig. 16 plots specific power (W kg<sup>-1</sup>) and specific energy (Wh kg<sup>-1</sup>) against capacity (kWh) for 37 kW systems.

A line indicating total system weight is included in Fig. 16 so that the characteristics of a 300 kg system (that is 30% the weight of a 1000 kg vehicle) can be easily identified.

Two systems were analysed in Fig. 16: a secondary system and a primary system (the weight of an on-board recharge device was left out). At 300 kg, the secondary system is projected to have a performance of 123 W kg<sup>-1</sup> and 91 Wh kg<sup>-1</sup>. A primary system at 300 kg projects to 124 W kg<sup>-1</sup> and 99 Wh kg<sup>-1</sup>. If fractions of vehicle weight in excess of 30% may be devoted to battery weight, significantly greater capacities than the 27 and 24 kWh projected here can be carried (though with some loss in power density).

Figure 17 presents a Ragoné plot of the analysis of the 1975 CGE system according to this modelling technique. A line depicting the model's projection for an improved system is included. A substantial range of system characteristics is available depending on the specific vehicle mission chosen.

The results of this modelling technique, the design of which was based on the real 1975 CGE 15 kW system, indicate that batteries performing

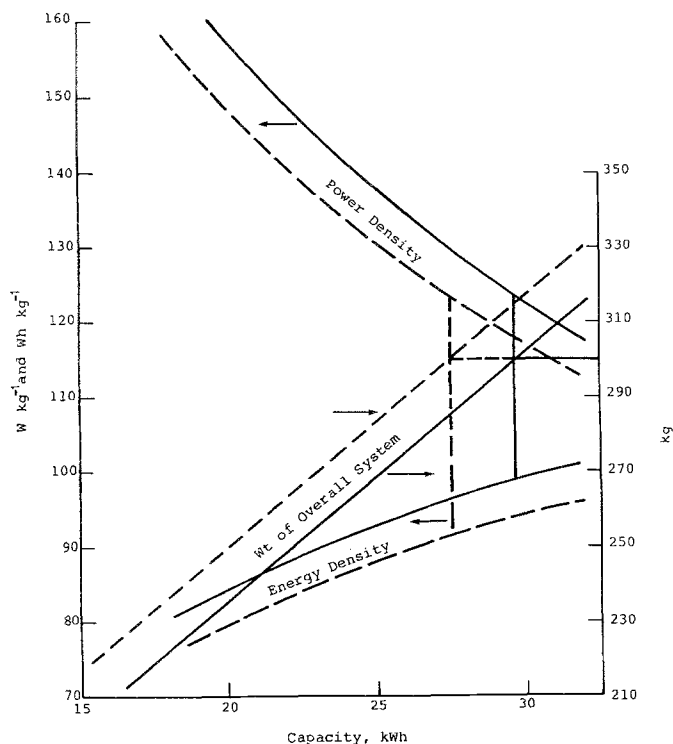


Fig. 16. Projection of primary and secondary vehicle battery characteristics —, primary system, --- secondary system.

near urban transportation requirements may be constructed.

### 7. Analysis of central recharge scenarios

Certain advantages to the economics of centrally recharged primary slurry zinc/air systems may be enumerated. First, the weight of the charge cells and d.c. power source may be removed from the vehicle and replaced by additional slurry electrolyte, thus improving vehicle range. Reprocessing zincate electrolyte to zinc slurry centrally would enjoy certain economies of scale, i.e. lower current densities and cell voltages may be used, and higher efficiencies in large-scale d.c. conversion would be available.

The energy content of a slurry of  $350 \text{ g dm}^{-3}$  of zinc in  $12 \text{ mol dm}^{-3}$  KOH is not sufficient to justify its transportation over great distances. The solution may be to reprocess at the sites at which spent electrolyte is off-loaded. Thus, one may envisage urban service stations in which spent electrolyte is pumped into a tank feeding a recharge electrolyser which then transfers reprocessed zinc slurry into a holding tank for return to the vehicle fleet. In such a scenario, transport of electrolyte is merely a matter of several

metres. Hydrogen may be piped from a central fossil fuel reforming plant.

Only in urban environments may the advantages of hydrogen depolarized recharge be utilized. Aside from an apparent advantage in primary-resource-to-road efficiency (to be

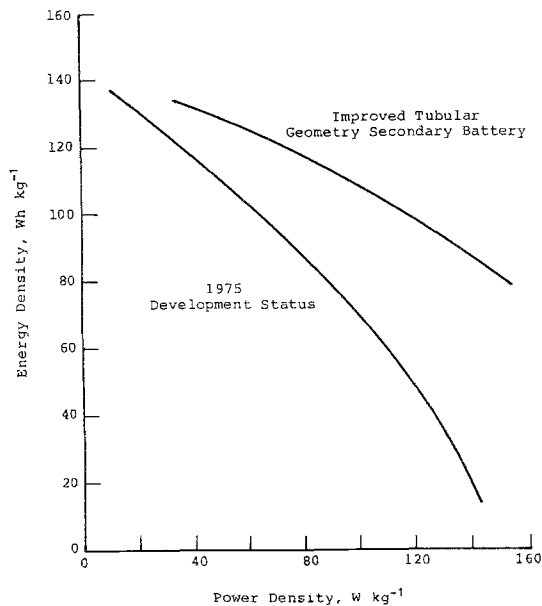


Fig. 17. Projection of range of system performance that may be designed.

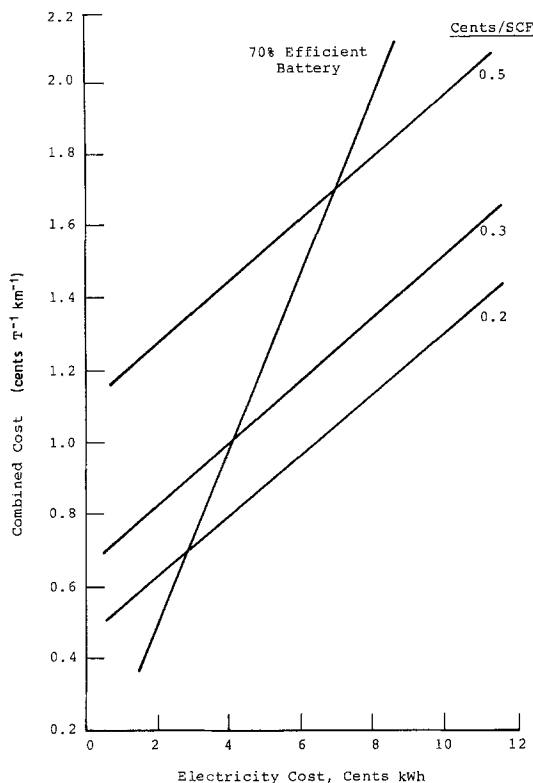


Fig. 18. Economic analysis of hydrogen depolarization in the recharge of slurry zinc/air systems.

outlined subsequently), an economic argument appears.

One may plot the cost per ton-kilometre of hydrogen-recharged slurry zinc/air transportation as a function of electricity cost at several different levels of hydrogen cost. Only a figure for an average  $\text{kWh km}^{-1}$  energy requirement for a 1000 kg vehicle is needed to construct such a plot. Figure 18 presents this analysis and also includes a cost line representing the use of a 70% electric-to-electric efficient battery (couple not specified). It can be seen that even at present costs of electricity and bulk hydrogen (6–8¢/kWh and 2–3¢/SCF) [20] the cost of hydrogen-recharged zinc/air transportation is approximately half that of using a 70% efficient conventional battery storage system.

## 8. Overall system efficiency

The energy efficiency of slurry zinc/air electric vehicles must be analysed separately for the case of oxygen-evolving recharge and hydrogen-

depolarized recharge. They must be put on an equivalent basis by extending the analysis back to fossil fuels.

### 8.1. Utilizing on-board recharge (evolving oxygen)

The overall electric-to-electric efficiency of the slurry zinc/air system may be calculated as the quotient of discharge voltage and charge voltage, multiplied by pumping losses (5% at cruise), self-discharge losses (0.7%), charging current efficiency losses (5%), and shunt current losses (5% at cruise). An average discharge voltage of 1.18 V is assigned, assuming an 11 kW average power demand (representing a discharge rate of  $80 \text{ mA cm}^{-2}$ ). A charge current density of  $150 \text{ mA cm}^{-2}$  corresponding to an 8 h overnight rate for a 10 kg small-scale charger gives a 2.4 V cell voltage. Thus, an electric-to-electric efficiency of 41.8% is projected for advanced slurry zinc/air systems.

To obtain a primary resource-to-road efficiency, for a comparison to syn-fuel propelled ICE vehicles, or a slurry zinc/air system recharged using hydrogen, the following factors must be taken into account. The generation of electric power from coal is at best 38% efficient. Distribution losses in the transmission of electricity average 9% [21]. When considering decentralized recharge, small d.c. power supplies also contribute a significant loss of 15%. Lastly, the efficiency of electric motors and their drivetrain must be multiplied in (78%) [21]. A 9.0% coal-to-road efficiency results. This figure may then be directly compared with that of alternative systems.

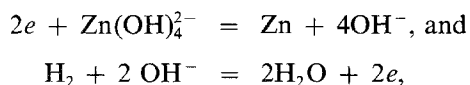
The best batteries under development for the EV application may have electric-to-electric efficiencies in the neighbourhood of 70%. This being the case, their coal-to-road efficiencies of 14.3% appear much more attractive than all metal/air systems (though their power and range are not always equivalent). Metal/air systems must be justified on the basis of higher performance than alternate batteries because their energy efficiencies have traditionally been thought of as low. If their efficiencies fall below that of internal combustion engine vehicles powered by coal-derived synthetic fuel, they are even less attractive.

This latter limit may be estimated as follows. An efficiency of 63% is projected for the hydrogenation of coal to liquid fuels [22]. This may be distributed with 99.6% efficiency. Coupling an engine efficiency of 20% and drive-train losses of 17%, an overall coal-to-road efficiency of 10.7% may be calculated. Such an efficiency appears greater than that of aluminium/air powered electric vehicles and oxygen-evolving recharge zinc/air systems. Methanol fuel cell [23] and ammonia/air [24] electric vehicle systems both have overall coal-to-road efficiencies of the order of 13.5%.

### 8.2. Utilizing hydrogen centrally

As an electric-to-electric efficiency cannot be spoken of in the case of hydrogen-depolarized reprocessing, a coal-to-road efficiency must be calculated, assuming both electric power and hydrogen are derived from coal or similar primary resources. Only the charge term need be replaced in the preceding analysis.

Charge efficiency is composed of two parts, accounting for energy from electric power and energy from the hydrogen anodically reacted. From the stoichiometry of the half-reactions:



and the projected charge cell voltage of 0.76 V at 75 mA cm<sup>-2</sup>, it can be calculated that 38.3% of the energy consumed in producing zinc comes from the electric power supplied and 61.8% comes from the hydrogen. The electricity fraction is subject to generation losses, distribution losses and losses in the electrochemical cell (0.42 V theoretical/0.76 V at the chosen rate). Efficiency of conversion to d.c. can be better than 95% in large (central) installations. Hydrogen may be generated from coal at approximately 65% efficiency. Thermal efficiencies for the steam reformation of methane are higher (74%), but steam reformations's 65% hydrogen efficiency is the appropriate number for this analysis [20]. An efficiency of 99% may be taken for local distribution.

When the charge and discharge terms are multiplied with the pumping, shunt current, self-discharge and electric drive system losses, an

overall primary resource-to-road efficiency of 15.9% results. Thus the use of hydrogen makes an enormous difference in both the economics and the overall efficiencies of the oxygen-evolving and hydrogen-depolarized recharge scenarios. Further analysis of the economics of large hydrogen plants and the capital cost of urban hydrogen distribution networks is necessary, much like in the case of the infrastructure requirements of the usage of the aluminium/air EV system as proposed at the Lawrence Livermore National Laboratory.

### 9. Difficulties foreseen in the development of slurry zinc/air systems

Some problems remain to be solved if slurry zinc/air batteries are ever to be used for vehicle propulsion. These may be broken down into headings of air cathode related problems, discharge cell design and construction, electrolyte properties and recharge methodology.

The problems of air cathodes are well-known, and need only be briefly described in relation to the slurry system. The problem of mechanical durability is not likely to be as severe in slurry zinc/air cells as in other applications, the active layer being compressed between exmets. However, they will be exposed to flowing electrolyte. Intermittent operation has not yet been completely studied. Maintenance procedures for CO<sub>2</sub> removal and possible zincate weeping have not yet been defined. Cathode cost is, of course, critical if noble metal catalysis is to be employed. A further practical problem lies in just how to apply or to seam seal air-cathodes if tubular cell geometry is chosen.

Discharge cell design is central to the optimization of power density. Current collection must be optimized in detail because the collection network accounts for over 90% of cell weight. In tubular geometry, the current collection issue determines what the length of the cells can be. The problem is essentially finding the maximum in the system power density as a function of increased current collector weight. Such an optimization may be performed by evaluating linear combinations of cross-sections of the individual components of the collection network.

Tubular cells are a particularly desirable configuration in that electrolyte flow characteristics may be precisely controlled. Tubular cells, however, are subject to difficulties in manufacture, and in front-to-rear electrolyte pressure variation.

Shunt currents are also a problem in common electrolyte systems. In the slurry zinc/air system, agglomerations of zinc will propagate in areas of potential gradient so that shorts and blockages result. Thus, zinc setting is a problem relating to more than just its utilization alone.

Other electrolyte-related problems can be discussed. The vapour pressure of water over  $12 \text{ mol dm}^{-3}$  KOH at  $55^\circ \text{C}$  indicates rebalancing steps will be necessary. Also, the discharge capacity of the electrolyte is strongly dependent on the concentration of the silicate additive. Variations of 10% too much or too little can reduce capacity by 50%. This capacity is also affected by discharge rate (current density) which is affected by anode current collector mesh size (which, in turn, affects system weight).

Pump design is another critical problem in that high recirculating-to-static volume ratios are required and that resistance to abrasion is essential. Due to shunt currents, non-metallic components are simultaneously necessary.

Problems to be overcome in the development of charging apparatus centre on the complete and reliable removal of electrodeposited zinc from magnesium substrates. Vibration, ultrasonic cavitation and shearing flow each work to varying degrees; however, a mechanical device may have to be engineered to (perhaps in one conception) draw a flexible scraper over the cathode surfaces. Incorporation of a fuel-cell-type electrode for the anodic oxidation of hydrogen does not simplify design problems.

## 10. Conclusions

With continued development it is possible that the slurry zinc/air system can meet the requirements of the electric vehicle application. The system's principle advantages are that of rapid mechanical recharge, simplicity and potential low cost. The possibility of improving the overall resource-to-road efficiency by a factor of two through the use of primary resource-derived

hydrogen in central recharge scenarios also deserves further exploration.

Development of slurry zinc/air technology can probably proceed rapidly as a good deal of scale-up engineering may be co-opted from previous development programmes [4–14, 25]. Also, valuable information such as air-cathode life and component system design, may become available from analogous work in the area of aluminium/air batteries.

Improvement in energy density, obtained through better colloidal suspension of discharge product, through discharge product separation, as well as through optimal system design, is indicated, though is not necessary to produce 300 to 350 kg systems of energy densities over  $100 \text{ Wh kg}^{-1}$ .

It is clear all the answers are not yet in hand, and that subsequent research on the slurry zinc/air couple is needed to critically evaluate some of the apparent advantages intrinsic to the system.

## Acknowledgements

The authors are grateful to Mr Mark L. Goodwin for his participation in the latter phases of the laboratory investigation.

## References

- [1] R. Witherspoon, E. Zeitner and H. Schulte, Proceedings of the Energy Conversion Engineering Conferences 71, (1971) 96–102.
- [2] P. Shipps, *Proc. Ann. Power Sources Conf.* **20** (1966) 86.
- [3] T. Chiku and K. Ninomiya, *Toyota Chuo Kenkyusho Kenkyu Hokoku* **73** (TR-3) (1973) 20.
- [4] 'Research and Development of Batteries for Electric Vehicles in Japan', Government Industrial Research Institute (1978).
- [5] H. Ikeda, N. Furukawa and M. Ide, 'Metal-Air Batteries', Sanyo Electric Co. Ltd., Osaka, Japan.
- [6] V. Maner and A. Nassalevska, 'Anodic Behavior of the Suspended Zinc Electrode', Laboratory of Electrochemical Power Sources, Bulgarian Academy of Sciences, Sofia, Bulgaria.
- [7] A. Appleby, J. Pompon and M. Jacquier, 'Economic and Technical Aspects of the CGE Zn-Air Vehicle Battery', *I.E.C.E.C. Record*, 8/75, 811.
- [8] A. Appleby and J. Gabano, 'Current status and prospects of the Zn-Air and Na-S batteries in France', in 'Proceedings of the Symposium and Workshop on Advanced Battery Research and Design', Argonne National Laboratory (1976).
- [9] A. Appleby and M. Jacquier, *J. Power Sources* **1** (1976/77) 17.
- [10] A. Appleby, J. Jacquelin and J. Pompon, 'Charge-



- Discharge Behavior of the CGE Circulating Zn-Air Vehicle Battery', Paper No. 770381, S.A.E. Congress and Exposition, Detroit (1977).
- [11] P. Durand, US Patent 4 133 940 (1979).
- [12] D. Doniat, US Patent 4 126 733 (1978).
- [13] F. Solomon and C. Grun, US Patent 4 147 839 (1976).
- [14] R. Remick and A. Sammells, 'Zinc/Air Batteries for Electric Vehicle Propulsion', Paper No. 112, 160th Meeting of the Electrochemical Society, Denver, Colorado (1981).
- [15] J. McBreen and E. Cairns, in 'Advances in Electrochemistry and Electrochemical Engineering' Vol. 11, Interscience, New York (1979).
- [16] A. Marshall and N. Hampson, *J. Electroanal. Chem.* **59** (1975) 19.
- [17] P. C. Foller, unpublished results.
- [18] Initial results, courtesy Prototech Co Newton Highlands, MA, USA.
- [19] J. F. Cooper, 'Weight and volume estimates for Al/air batteries designed for E.V. applications', 'Proceedings 1st International Workshop on Reactive Metal/Air Batteries', Bonn (1979).
- [20] The Changing Economics of Hydrogen, *Chemical Week* **134** (1982) 42.
- [21] J. Salisbury, E. Behrin, M. Kong and D. Whisler, 'A Comparative Analysis of Aluminium/Air Battery Propulsion Systems for Passenger Vehicle', Lawrence Livermore Laboratory, UCRL-52933 (1980).
- [22] E. Dickson, et al., 'Synthetic Liquid Fuels Development: Assessment of Critical Factors', ERDA **4** (1977) p. 76.
- [23] T. Benjamin, E. Camara and L. Marianowski, 'Handbook of Fuel Cell Performance', DOE COO-1545-TI (1980).
- [24] P. N. Ross, 'Characteristics of an NH<sub>3</sub>/air fuel cell system for vehicular application', 'Proceedings, ASME 16th IECEC Conference', Atlanta (1981).
- [25] P. C. Foller and D. E. Stephens, 'Imposed Slurry Zinc/Air Systems as Secondary Batteries for Vehicle Propulsion', Paper No. 113, 160th meeting of the Electrochemical Society, Denver, Colorado (1981).